Asymmetric Loop Spectra and Unbroken Phase Protection due to Nonlinearities in $\mathcal{PT}$-Symmetric Periodic Potentials

Yongping Zhang,[1,*] Zhu Chen,[2] Biao Wu,[3,4,5] Thomas Busch,[6] and Vladimir V. Konotop[7,†]

[1]International Center of Quantum Artificial Intelligence for Science and Technology (QuArtist) and Department of Physics, Shanghai University, Shanghai 200444, China
[2]Institute of Applied Physics and Computational Mathematics, Beijing 100094, China
[3]International Center for Quantum Materials, School of Physics, Peking University, Beijing 100871, China
[4]Wilczek Quantum Center, School of Physics and Astronomy, Shanghai Jiao Tong University, Shanghai 200240, China
[5]Collaborative Innovation Center of Quantum Matter, Beijing 100871, China
[6]Quantum Systems Unit, Okinawa Institute of Science and Technology Graduate University, Okinawa 904-0495, Japan
[7]Centro de Física Teórica e Computacional and Departamento de Física, Faculdade de Ciências, Universidade de Lisboa, Campo Grande 2, Edifício C8, Lisboa 1749-016, Portugal

(Received 19 February 2021; accepted 15 June 2021; published 13 July 2021)

We demonstrate that the interplay between a nonlinearity and $\mathcal{PT}$ symmetry in a periodic potential results in peculiar features of nonlinear periodic solutions. These include thresholdless symmetry breaking and asymmetric (multi-)loop structures of the nonlinear Bloch spectrum, persistence of unbroken $\mathcal{PT}$ symmetry even after the gap is closed, nonmonotonic dependence of the $\mathcal{PT}$ phase transition on the defocusing nonlinearity, and enhanced stability of the nonlinear states corresponding to the loop structures. The asymmetry and the loop structure of the spectrum are explained within the framework of a two-mode approximation and an effective potential theory and are validated numerically.

DOI: 10.1103/PhysRevLett.127.034101

Controlling the properties of propagating waves in synthetic materials is a topic of fundamental and applied interest. Traditionally, periodic modulations of parameters of the guided media is considered as one of the main tools of such control. More recently, a possibility of combining nonconservative effects with periodicity of the medium parameters [1,2], especially when the non-Hermiticity features parity-time ($\mathcal{PT}$) symmetry [3,4], has become a topic of intense study, with a particular interest in optical settings where they can be realized by periodically modulating a complex dielectric permittivity [5–9]. While the properties of linear $\mathcal{PT}$-symmetric lattices are, by now, well understood [10–12], a broad range of applications in diverse areas of physics have also stimulated studies of the effects of nonlinearities in $\mathcal{PT}$-symmetric systems [13–15].

If the periodic $\mathcal{PT}$-symmetric potential itself is linear, the inclusion of nonlinearities has, for example, led to the description of nonlinear periodic waves [6,16], solitons [5,6,17–19], and defect modes [20,21]. All these effects were observed when the underlying linear system is in the unbroken $\mathcal{PT}$-symmetric phase [3], illustrating that properties of systems obeying $\mathcal{PT}$ symmetry resemble behavior of Hermitian systems [13].

In linear systems, spontaneous $\mathcal{PT}$ symmetry breaking can be viewed as an instability under a change of parameters and is signaled by the emergence of complex eigenvalues in the spectrum. At the same time, instabilities are also inherent features of nonlinear systems, even Hermitian ones. Similarly, these instabilities occur through a transition between phases characterized by pure real and complex spectra (corresponding to stable and unstable nonlinear modes), but in this case, for the eigenvalue problem of small excitations of the nonlinear modes. The Bogoliubov-de Gennes equations for a Bose-Einstein condensate (BEC) are a celebrated description of this and the stability analysis of periodic nonlinear waves in conservative linear lattices has, for example, been discussed in [22–25].

The presence of non-Hermiticity in a nonlinear eigenvalue problem is, therefore, an interesting setting to study the effects of nonlinearity on $\mathcal{PT}$ symmetry breaking in periodic potentials [26], now understood as emergence of complex eigenvalues of a nonlinear eigenvalue problem and, also, the opposite effect of non-Hermiticity on the stability of nonlinear modes. In Hermitian systems, sufficiently strong nonlinearities can lead to a change in the topology of the spectrum of the respective nonlinear periodic waves. It was shown, in a series of theoretical works [27–34], that the nonlinear spectrum of the nonlinear

Bloch modes in an atomic BEC (a nonlinear Hermitian eigenvalue problem) can feature a loop structure, whose presence has also already been experimentally observed [35–37]. A loop spectrum is also predicted for nonlinear Bloch states in exciton-polariton condensates [38].

In this Letter, we show that the loop spectrum acquires new properties in the presence of non-Hermiticity. The combination of $\mathcal{PT}$ symmetry and nonlinearity leads to the nonlinear Bloch spectrum becoming asymmetric with respect to Brillouin zone (BZ) center or edges. In the presence of loops, this asymmetry is reflected in the tilt of the loops with respect to the BZ edges. In fact, the tilted loops can connect the relevant bands and, thereby, bridge the energy gap. However, even in the presence of a closed gap, the system is still in the unbroken phase, what is starkly different from cases of linear $\mathcal{PT}$ symmetry and nonlinear $\mathcal{PT}$ symmetry without loop structures. In both of these cases closing the energy gap pushes the system into the broken phase. Furthermore, the extension of the unbroken phase is guaranteed by the tilted loops independent of the nonlinearity being focusing or defocusing. To give an intuitive physics picture for understanding the effects, we present an effective potential theory describing nonlinear $\mathcal{PT}$ phase transition in the absence and presence of loop structures.

Bearing in mind applications in paraxial optics, we consider the scaled nonlinear Schrödinger (NLS) equation

$$i\psi_z = H_{\mathrm{lin}}\psi + c|\psi|^2\psi, \qquad H_{\mathrm{lin}} = -\frac{1}{2}\partial_x^2 + V(x). \tag{1}$$

Here, ψ is the dimensionless field amplitude, z is the propagation distance measured in the units $4n_0\ell/\lambda_0$, x is the transverse coordinate in the units of ℓ/π, n_0 is the refractive index of the homogeneous medium modulated by the complex grating $\Delta n(x)$ with the period ℓ, and λ_0 is the light wavelength. The optical potential is defined by $V(x) = -8(\ell^2/\lambda^2)n_0\Delta n(x)$ and in the chosen scaling satisfies the properties $V(x) = \mathcal{PT}V(x) = V^*(-x) = V(x+\pi)$. The real-valued nonlinear coefficient $c = -4\pi n_0 n_2 P_0 \ell$, with n_2 being the Kerr nonlinearity and P_0 being the power of the incident light, describes either defocusing ($c > 0$) or focusing ($c < 0$) media. Typical physical parameters correspond to wavelengths λ_0 on the order of one micron, grating periods of about ten microns, and grating amplitudes on the order of 10^{-3} (see, e.g., [39]). We are interested in solutions of the form $\psi(z,x) = e^{i\beta_k z + ikx}\phi_k(x)$, often referred to as nonlinear Bloch waves, where β_k is a propagation constant, k is the Bloch vector, and $\phi_k(x)$ is a periodic function, $\phi_k(x) = \phi_k(x+\pi)$, solving the stationary NLS equation

$$\beta_k\phi_k + H_k\phi_k + c|\phi_k|^2\phi_k = 0, \quad H_k = -\frac{1}{2}(\partial_x + ik)^2 + V(x). \tag{2}$$

We are interested in studying the dependence of stationary solutions on the nonlinearity parameter c when fixing the normalization of the (nonlinear) eigenmodes as $\langle\phi_k, \phi_k\rangle = 1$, where the internal product defined by $\langle f, g\rangle = (1/\pi)\int_0^\pi f^*(x)g(x)dx$.

Thresholdless nonlinear symmetry breaking.—The real part of the spectrum of the linear eigenvalue problem $\tilde{\beta}_k\tilde{\phi}_k + H_k\tilde{\phi}(x) = 0$ is symmetric [7–9], i.e., $\tilde{\beta}_k = \tilde{\beta}_{-k}$ [hereafter we use the tilde to denote the solutions of the underlying linear problem, i.e., of (2) at $c = 0$]. However, even an infinitesimal nonlinearity ($c \neq 0$) breaks this symmetry and leads to $\beta_k \neq \beta_{-k}$. This can be shown by considering the bifurcation of a nonlinear family of periodic solutions from the linear one. Setting $|c| \ll 1$, we look for the nonlinear solution of (2) in the form of expansions $\beta_k = \tilde{\beta}_k + c\beta_k^{(1)} + \cdots$ and $\phi_k = \tilde{\phi}_k + c\phi_k^{(1)} + \cdots$. Defining the eigenstates φ_k of the Hermitian conjugate $H_k^\dagger$ and assuming that the spectrum of H_k is free from exceptional points, we, thus, have a biorthogonal basis $\{\varphi_k, \tilde{\phi}_k\}: \langle\varphi_k, \tilde{\phi}_{k'}\rangle = 0$ for $k \neq k'$. Now, suppose that, for a given Bloch vector k, the eigenvalue $\tilde{\beta}_k$ is real. Then, one can choose $\varphi_k = \tilde{\phi}_k^*$ and compute $\beta_k^{(1)} = \langle\tilde{\phi}_k^*, |\tilde{\phi}_k|^2\tilde{\phi}_k\rangle / \langle\tilde{\phi}_k^*, \tilde{\phi}_k\rangle$. Since $H_{-k} \neq H_k$, and hence, $\tilde{\phi}_{-k} \neq \tilde{\phi}_k$, we conclude that, in a generic case, $\beta_k^{(1)} \neq \beta_{-k}^{(1)}$. While this last condition does not exclude the possibility of an accidental coincidence of $\beta_k^{(1)}$ and $\beta_{-k}^{(1)}$, the equality of the propagation constants at k and $-k$ would require exact coincidence of corrections in all orders of the expansion. This leads us to the conclusion that $\beta_k \neq \beta_{-k}$. It is worth noting that, if H_k is Hermitian, i.e., if $V(x)$ is real, then one can set $\varphi_k = \tilde{\phi}_{-k}^* = \tilde{\phi}_k$. This choice replaces the biorthogonal basis by the standard basis of the Bloch states $\{\tilde{\phi}_k\}$, and one recovers the known result that $\beta_k^{(1)} = \beta_{-k}^{(1)}$, i.e., in this case the nonlinearity does not break the symmetry of the spectrum.

Shallow lattice regime.—Spontaneous nonlinear symmetry breaking can be explicitly illustrated in the limit of a shallow lattice in the weakly nonlinear regime where the two-mode approximation [27] is valid. To this end, we address the known potential [5,6,9,11,39]

$$V(x) = \mathrm{V}\left[\cos^2(x) + i\frac{\mathrm{V}_0}{2}\sin(2x)\right], \tag{3}$$

that in the linear limit (at $c = 0$) supports unbroken [$\tilde{\beta}_k$ is real for $k \in [-1, 1)$] and broken ($\tilde{\beta}_k$ acquires complex values in the BZ) $\mathcal{PT}$-symmetric phases for $\mathrm{V}_0 < 1$ and $\mathrm{V}_0 > 1$, respectively. If $\mathrm{V} \ll 1$ and $c = \mathrm{V}c'$ where $|c'| \sim 1$, the spectrum near the band edge at $k = 1 + \mathrm{V}\delta$, where $\mathrm{V}\delta$ is a small displacement of quasimomentum from the BZ edge, can be described by accounting only for two modes resonantly coupled by the Bragg scattering. Respectively, in the unbroken phase, we look for a Bloch state of the form

$\phi_k(x) \approx a_{-1}e^{-2ix} + a_0$ where $a_{0,-1}$ are real constants satisfying $a_0^2 + a_{-1}^2 = 1$. Defining $\boldsymbol{a} = (a_{-1}, a_0)^T$ (T stands for transpose), we obtain the nonlinear eigenvalue problem $h(\boldsymbol{a})\boldsymbol{a} = \delta\boldsymbol{a}$, where the effective non-Hermitian Hamiltonian is given by $h(\boldsymbol{a}) = \nu\sigma_3 + (1/4)(\sigma_1 \mathrm{V}_0 + i\sigma_2) - (c'/2)\sigma_3\boldsymbol{a}^\dagger\sigma_3\boldsymbol{a}$ (here, $\sigma_{1,2,3}$ are the Pauli matrices) and $\nu = -[(2\beta+1)/\mathrm{V} + \mathrm{V}\delta^2 + 3c' + 1]/2$. The dispersion relation is obtained in the form [40]

$$\nu^4 + \nu^3 c' + \nu^2\left(\frac{c'^2}{4} - \delta^2 - \frac{1}{16} + \frac{\mathrm{V}_0^2}{8}\right) - \nu\frac{c'}{16}(1 - \mathrm{V}_0^2) + \frac{\mathrm{V}_0^2}{16}\left(\frac{\mathrm{V}_0^2}{16} - \delta^2 - \frac{1}{16}\right) + \frac{\mathrm{V}_0 c'\delta}{16} - \frac{c'^2}{64} = 0, \tag{4}$$

which for $\mathrm{V}_0 = 0$ recovers the result of [27]. This expression contains several important results. First, in the linear limit of $c' = 0$, the resulting quartic equation has two real-valued solutions at $\delta = 0$ which define the energy gap $E_{\mathrm{gap}} = \mathrm{V}(1 - \mathrm{V}_0^2)^{1/2}/2$. Thus, we recover the well-known result that the gap is closed at $\mathrm{V}_0 = 1$. Second, if either $\mathrm{V}_0 = 0$ (Hermitian case) or $c = 0$ (linear case), the dispersion relation is symmetric, i.e., the propagation constant depends on δ^2. If, however, $c\mathrm{V}_0 \neq 0$ one can see that $\beta'(\delta) \neq \beta'(-\delta)$, which means that the symmetry with respect to the center of the BZ is broken. Thus, in agreement with the above considerations in a deep lattice, we conclude that the spontaneous symmetry breaking of the dispersion relation requires the simultaneous presence of a nonlinearity and non-Hermiticity. Third, at $c' = c_b$, where

$$c_b = \frac{\mathrm{V}_0(\sqrt{8\mathrm{V}_0^2 + 1} - 4\mathrm{V}_0^2 + 1)}{2[2(1 - \mathrm{V}_0^2)(\sqrt{8\mathrm{V}_0^2 + 1} - 2\mathrm{V}_0^2 - 1)]^{1/2}}, \tag{5}$$

there exist one simple and one triple root of (4). This occurs at

$$\delta_b^2 = (\sqrt{8\mathrm{V}_0^2 + 1} - 2\mathrm{V}_0^2 - 1)/[32(1 - \mathrm{V}_0^4)], \tag{6}$$

with $\mathrm{sign}(\delta) = \mathrm{sign}(c)$, and means that c_b is the bifurcation point at which a loop appears in the spectrum. Notice that, unlike in the Hermitian case [27,30–32,34], the loop now bifurcates from a point shifted away from the BZ edge. At $|c'| > c_b$ there exist four real solutions of (4) for a given δ in the vicinity of δ_b, corresponding to the loop. Finally, solving (4) with respect to δ for a given ν, one finds that the roots $\delta^{(1,2)}$ exist only for $\nu^2 \geq 1/4(1 - \mathrm{V}_0^2)$, i.e., below the critical value $\mathrm{V}_0 = 1$ there exist three values of ν at which $\delta^{(1)} = \delta^{(2)}$. Thus, at these parameters loop crossing occurs, which is a genuinely non-Hermitian phenomenon.

Loop structure and $\mathcal{PT}$ symmetry breaking.—Now, we proceeded with a full numerical analysis. In Fig. 1, we show the nonlinear Bloch spectrum for defocusing (upper row) and focusing (lower row) interactions. For defocusing (focusing) interactions, one can see the loop bifurcating from the upper (lower) band, and in the Hermitian case ($\mathrm{V}_0 = 0$), the loop is symmetric with respect to the BZ center $k = 0$ and edges $k = \pm 1$ [see Fig. 1(a1)]. At the critical point, just before the appearance of a loop, the spectrum develops a cusp structure, and we show an example of this in Fig. 1(b1).

In the presence of a complex lattice, $\mathrm{V}_0 \neq 0$, and for finite nonlinearity, the loop structures lose their symmetry with respect to either $k = 0$ or $k = \pm 1$, which is confirmed in Figs. 1(a2) and 1(b2). The presence of an imaginary part in the lattice tilts the loops toward the right (left) sides of BZ edges for defocusing (focusing) interactions when the

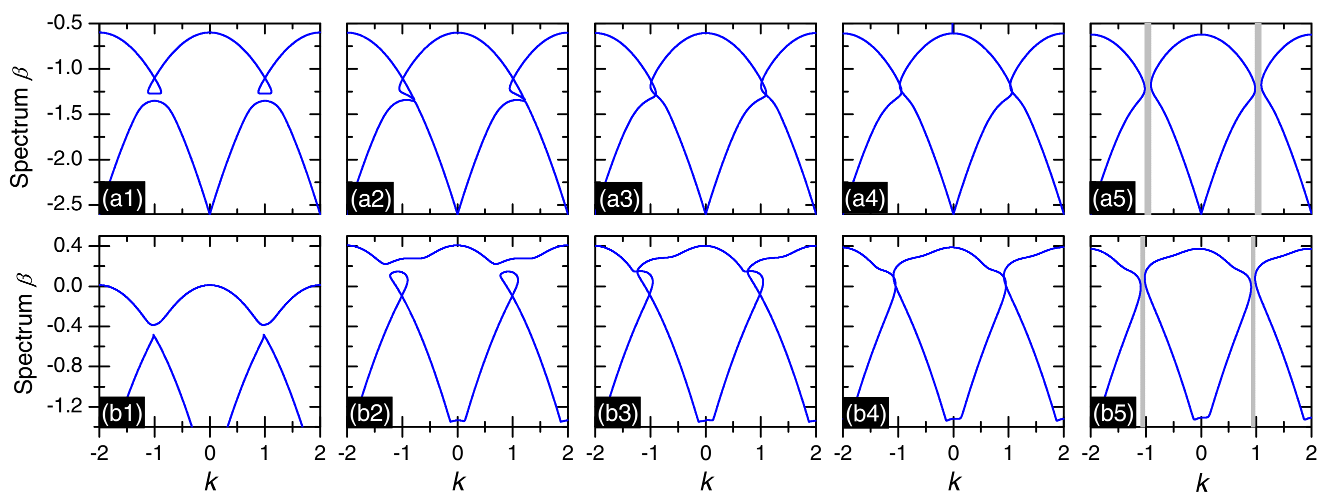

FIG. 1. The loop structure of the nonlinear Bloch spectrum for defocusing $c = 0.5$ (upper row) and focusing $c = -0.5$ [lower row, (b2)–(b5)] interactions for $\mathrm{V} = 0.2$. Only the highest two Bloch bands are shown. The panels in the upper and lower rows from left to right correspond to $\mathrm{V}_0 = \{0, 0.8, 1.6, 2, 3\}$ and $\mathrm{V}_0 = \{0.4, 0.8, 1.6, 3, 3.8\}$, respectively. The panel (b1) shows a cusp under the critical coefficient c_b from Eq. (5). In the shaded areas in panels (a5) and (b5), the spectrum is complex, i.e., $\mathcal{PT}$ symmetry is broken.

sign of V_0 is positive, and vice versa [40]. The asymmetry of the loop structures becomes more pronounced with increasing values of V_0, which ultimately leads to the loops connecting the respective neighboring bands [see Figs. 1(a2) and 1(b3)]. One can also see from Figs. 1(a3), 1(a4), 1(b3), and 1(b4) that the areas inside the loops that connect the lowest two bands shrink with increasing values of V_0. Once the area goes to zero, complex eigenvalues appear, indicated by the shaded regions in Figs. 1(a5) and 1(b5) [these regions are beyond the applicability of the two-mode approximation, as Eq. (4) does not admit a fourth-order root].

This $\mathcal{PT}$ phase transition occurs at a critical strength of the imaginary part of the lattice, V_0^c, that depends on the strength of the nonlinearity. This dependence is shown Figs. 2(a) and 2(b) for two typical values of V. A general observation is that focusing interactions suppress the $\mathcal{PT}$ phase transition by increasing V_0^c to values larger than 1 (this recovers the conclusion of Ref. [26]). However, for the defocusing interactions shown in Figs. 2(a) and 2(b), we observe two different behaviors. For increasing nonlinearity, V_0^c initially decreases until it reaches a minimal value, after which it increases. Further increasing c, therefore, leads to an increase of V_0^c, which corresponds to an enhancement of the unbroken $\mathcal{PT}$-symmetric phase (this effect was not noticed in [26]). In fact, at some value of the nonlinear coefficient, denoted by c_T, the linear threshold $V_0^c = 1$ is restored [see vertical dotted line in Fig. 2(b)], with the magnitude of the threshold value depending on the depth of the real lattices as shown in Fig. 2(c). A smaller V requires a smaller c_T to observe the enhancement.

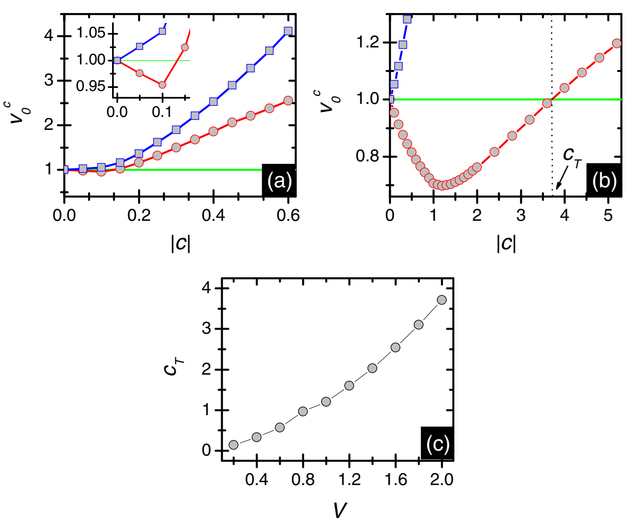

FIG. 2. Critical values of the depth of the imaginary part of the lattice for the $\mathcal{PT}$ symmetry phase transition. In (a) (V = 0.2) and (b) (V = 2), squares and circles correspond to the cases of focusing and defocusing interactions, respectively. The horizontal lines at $V_0^c = 1$ indicate the linear $\mathcal{PT}$ transition critical value. The inset in (a) shows details of the curves for small nonlinearities. (c) Threshold value c_T as a function of V for defocusing interactions. Beyond the threshold value the defocusing interactions protect the $\mathcal{PT}$ unbroken phase.

To provide physical insight into the different behaviors of V_0^c in the two regimes, we recall that, in the linear case, the phase transition is determined by the relation between the amplitudes of the real and imaginary parts of the lattice. However, in the presence of a nonlinearity, one can consider an effective potential, $V_{\rm eff} = \mathrm{V}\cos^2(x) + c|\phi_k(x)|^2$, which means one now has to consider the difference of the amplitudes of the effective real lattices potential $V_{\rm eff}$ and the imaginary lattice. In the weakly nonlinear regime, $\mathrm{V}\cos^2(x)$ dominates $V_{\rm eff}$, which leads to a preference to localize the density in the lattice sites. However, increasing the defocusing interactions, $c > 0$ leads to an extension of the density in space, which reduces the depth of the effective lattice potential. Thus, the effective lattice is weakened by the defocusing interactions, and the $\mathcal{PT}$ symmetry breaking threshold decreases [see Figs. 2(a) and 2(b)]. On the other hand, a focusing interaction ($c < 0$) tends to increase the effective lattice amplitude and, hence, results in an increase of the $\mathcal{PT}$ symmetry breaking threshold. In the opposite limit of strong nonlinearity, the linear lattice becomes a small correction to $V_{\rm eff} \propto c|\phi_k(x)|^2$. Independent of the sign of c, the effective lattice becomes much larger than the imaginary one, and the $\mathcal{PT}$ symmetry is restored independently of whether the interactions are focusing or defocusing.

On experimental observation.—To experimentally observe the reported asymmetry of the loop spectrum, one can focus on two features of the system. First, the reported states feature transverse currents [see, e.g., the phases in Fig. 3(b)] dependent on the strength of the gain and loss responsible for the $\mathcal{PT}$-symmetric landscape of the dielectric permittivity. Second, in systems with defocusing interactions, the Bloch states around the BZ edges in the lowest Bloch band are modulationally unstable in the absence of spectral loops (this was shown for nonlinear Bloch modes in BECs [16,22,41–45]). The loops can stabilize nearby Bloch states. We have examined the stability of the Bloch states in the presence of asymmetric loop structures using the standard linear stability analysis. A typical result is shown in Fig. 3(a), where the Bloch states that are found to be stable (unstable) are represented by thick red (thin blue) lines. Notice that the stability of nonlinear states is confirmed for opposite propagating waves corresponding to the same Bloch wave number k but having different depth of the density modulations [illustrated in Fig. 3(b)]. To confirm the stability in the direct propagation, we calculated the evolution of Bloch states, like the ones illustrated in Fig. 3(b), perturbed at the input by noise of order of 10% of the mode amplitude. The case examples of such evolution are shown in Figs. 3(c) and 3(d). In panel 3(d), we observe stable evolution of a Bloch state [labeled by “c” in Fig. 3(a)] over very long distances,

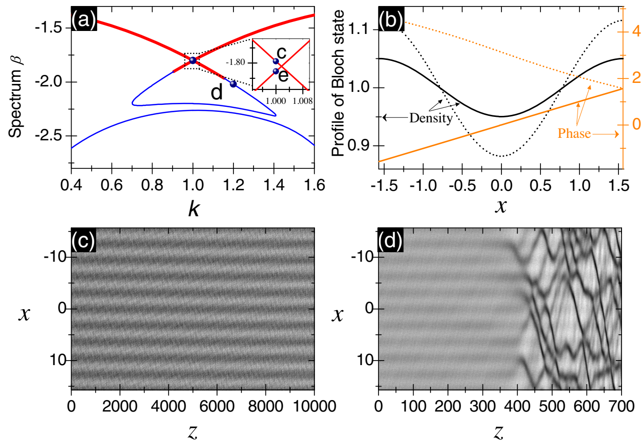

FIG. 3. Loop protected modulational stability for a system with $c = 1.2$, $V = 0.2$, and $V_0 = 0.4$. (a) Bloch spectrum around BZ edge $k = 1$. Nonlinear states corresponding to the thick red (thin blue) lines are modulationally stable (unstable). The inset shows details of the point $k = 1$. (b) Densities and phases of Bloch states at $k = 1$ shown over one period. The solid (dashed) lines correspond to the Bloch state labeled by "c" ("e") in (a). (c), (d) Nonlinear evolution of Bloch states with 10% random noise added initially into the Bloch states. In (c), the stable Bloch state at $k = 1$ corresponds to the one labeled by "c" in (a). In (d), the unstable Bloch state at $k = 1.2$ corresponds to the one labeled by "d" in (a). Note the difference in length scales z in (c),(d).

whereas an unstable mode [labeled by "d" in Fig. 3(a)] quickly loses its structure as shown Fig. 3(d). Note that the stable regimes in Fig. 3(a) are not symmetric with respect to the BZ edge at $k = 1$, which is due to the asymmetry of the loop structure.

In conclusion, we have shown that the simultaneous presence of a nonlinearity and $\mathcal{PT}$ symmetry of a linear periodic potential leads to unusual properties of nonlinear Bloch states. The nonlinear Bloch spectrum allows for thresholdless symmetry breaking, that does not occur if only one of the above factors is present. We have shown that, for sufficiently large nonlinearities, the spectrum acquires loop structures, which can bridge the energy gap and connect the highest two Bloch bands without a $\mathcal{PT}$ phase transition occurring. In the vicinity of the points from which the loops originate, the periodic solutions in the case of defocusing nonlinearity are stable and feature transverse currents, what make them experimentally observable.

We acknowledge useful discussions with Yong Xu. This work was supported by the Okinawa Institute of Science and Technology Graduate University. Y. Z. is supported by the National Natural Science Foundation of China (Grants No. 11974235 and No. 11774219) and Shanghai Municipal Science and Technology Major Project (Grant No. 2019SHZDZX01-ZX04). B. W. is supported by the National Key R&D Program of China (Grants No. 2017YFA0303302 and No. 2018YFA0305602), National Natural Science Foundation of China (Grant No. 11921005), and Shanghai Municipal Science and Technology Major Project (Grant No. 2019SHZDZX01). V. V. K. acknowledges financial support from the Portuguese Foundation for Science and Technology (FCT) under Contracts No. UIDB/00618/2020 and No. PTDC/FIS-OUT/3882/2020.

*yongping11@t.shu.edu.cn
†vvkonotop@fc.ul.pt

[1] M. V. Berry, Lop-sided diffraction by absorbing crystals, J. Phys. A **31**, 3493 (1998).
[2] C. M. Bender, G. V. Dune, and P. N. Meisinger, Complex periodic potentials with real band spectra, Phys. Lett. A **252**, 272 (1999).
[3] C. M. Bender and S. Boettcher, Real Spectra in Non-Hermitian Hamiltonians Having $\mathcal{PT}$ Symmetry, Phys. Rev. Lett. **80**, 5243 (1998).
[4] C. M. Bender, Making sense of non-Hermitian Hamiltonians, Rep. Prog. Phys. **70**, 947 (2007).
[5] Z. H. Musslimani, K. G. Makris, R. El-Ganainy, and D. N. Christodoulides, Optical Solitons in $\mathcal{PT}$ Periodic Potentials, Phys. Rev. Lett. **100**, 030402 (2008).
[6] Z. H. Musslimani, K. G. Makris, R. El-Ganainy, and D. N. Christodoulides, Analytical solutions to a class of nonlinear Schrödinger equations with $\mathcal{PT}$-like potentials, J. Phys. A **41**, 244019 (2008).
[7] S. Longhi, Bloch Oscillations in Complex Crystals with $\mathcal{PT}$ Symmetry, Phys. Rev. Lett. **103**, 123601 (2009).
[8] S. Longhi, Spectral singularities and Bragg scattering in complex crystals, Phys. Rev. A **81**, 022102 (2010).
[9] K. G. Makris, R. El-Ganainy, D. N. Christodoulides, and Z. H. Musslimani, $\mathcal{PT}$-symmetric optical lattices, Phys. Rev. A **81**, 063807 (2010).
[10] P. Djakov and B. S. Mityagin, Instability zones of periodic 1-dimensional Schrödinger and Dirac operators, Russ. Math. Surv. **61**, 663 (2006).
[11] B. Midya, B. Roy, and R. Roychoudhury, A note on the $\mathcal{PT}$ invariant periodic potential $V(x) = 4\cos^2 x + 4iV_0 \sin 2x$, Phys. Lett. A **374**, 2605 (2010).
[12] E.-M. Graefe and H. F. Jones, $\mathcal{PT}$-symmetric sinusoidal optical lattices at the symmetry-breaking threshold, Phys. Rev. A **84**, 013818 (2011).
[13] V. V. Konotop, J. Yang, and D. A. Zezyulin, Nonlinear waves in $\mathcal{PT}$-symmetric systems, Rev. Mod. Phys. **88**, 035002 (2016).
[14] S. V. Suchkov, A. A. Sukhorukov, J. Huang, S. V. Dmitriev, C. Lee, and Y. S. Kivshar, Nonlinear switching and solitons in $\mathcal{PT}$-symmetric photonic systems, Laser Photonics Rev. **10**, 177 (2016).
[15] *Parity-Time Symmetry and its Applications*, edited by D. Christodoulides and J. Yang, Springer Tracts in Modern Physics Vol. 280 (Springer, Berlin, 2018), https://www.springer.com/gp/book/9789811312465#aboutAuthors.
[16] F. K. Abdullaev, V. V. Konotop, M. Salerno, and A. V. Yulin, Dissipative periodic waves, solitons, and breathers of the nonlinear Schrödinger equation with complex potentials, Phys. Rev. E **82**, 056606 (2010).

[17] X. Zhu, H. Wang, L.-X. Zheng, H. Li, and Y.-J. He, Gap solitons in parity-time complex periodic optical lattices with the real part of superlattices, Opt. Lett. **36**, 2680 (2011).

[18] S. Nixon, L. Ge, and J. Yang, Stability analysis for solitons in $\mathcal{PT}$-symmetric optical lattices, Phys. Rev. A **85**, 023822 (2012).

[19] S. Nixon, Y. Zhu, and J. Yang, Nonlinear dynamics of wave packets in parity-time-symmetric optical lattices near the phase transition point, Opt. Lett. **37**, 4874 (2012).

[20] K. Zhou, Z. Guo, J. Wang, and S. Liu, Defect modes in defective parity-time symmetric periodic complex potentials, Opt. Lett. **35**, 2928 (2010).

[21] Z. Lu and Z.-M. Zhang, Defect solitons in parity-time symmetric superlattices, Opt. Express **19**, 11457 (2011).

[22] J. C. Bronski, L. D. Carr, B. Deconinck, J. N. Kutz, and K. Promislow, Stability of repulsive Bose-Einstein condensates in a periodic potential, Phys. Rev. E **63**, 036612 (2001).

[23] J. C. Bronski, L. D. Carr, R. Carretero-González, B. Deconinck, J. N. Kutz, and K. Promislow, Stability of attractive Bose-Einstein condensates in a periodic potential, Phys. Rev. E **64**, 056615 (2001).

[24] G. L. Alfimov and A. I. Avramenko, Coding of nonlinear states for the Gross–Pitaevskii equation with periodic potential, Physica (Amsterdam) **254D**, 29 (2013).

[25] G. L. Alfimov, P. P. Kizin, and D. A. Zezyulin, Gap solitons for the repulsive Gross-Pitaevskii equation with periodic potential: Coding and method for computation, Disc. Cont. Dyn. Sys. B **22**, 1207 (2017).

[26] Y. Lumer, Y. Plotnik, M. C. Rechtsman, and M. Segev, Nonlinearly Induced $\mathcal{PT}$ Transition in Photonic Systems, Phys. Rev. Lett. **111**, 263901 (2013).

[27] B. Wu and Q. Niu, Nonlinear Landau-Zener tunneling, Phys. Rev. A **61**, 023402 (2000).

[28] J. Liu, L. Fu, Bi-Y. Ou, S. G. Chen, D.-Il Choi, B. Wu, and Q. Niu, Theory of nonlinear Landau-Zener tunneling, Phys. Rev. A **66**, 023404 (2002).

[29] E. J. Mueller, Superfluidity and mean-field energy loops: Hysteretic behavior in Bose-Einstein condensates, Phys. Rev. A **66**, 063603 (2002).

[30] D. Diakonov, L. M. Jensen, C. J. Pethick, and H. Smith, Loop structure of the lowest Bloch band for a Bose-Einstein condensate, Phys. Rev. A **66**, 013604 (2002).

[31] M. Machholm, C. J. Pethick, and H. Smith, Band structure, elementary excitations, and stability of a Bose-Einstein condensate in a periodic potential, Phys. Rev. A **67**, 053613 (2003).

[32] B. T. Seaman, L. D. Carr, and M. J. Holland, Nonlinear band structure in Bose-Einstein condensates: Nonlinear Schrödinger equation with a Kronig-Penney potential, Phys. Rev. A **71**, 033622 (2005).

[33] I. Danshita and S. Tsuchiya, Stability of Bose-Einstein condensates in a Kronig-Penney potential, Phys. Rev. A **75**, 033612 (2007).

[34] G. Watanabe, S. Yoon, and F. Dalfovo, Swallowtail Band Structure of the Superfluid Fermi Gas in an Optical Lattice, Phys. Rev. Lett. **107**, 270404 (2011).

[35] Y.-A. Chen, S. D. Huber, S. Trotzky, I. Bloch, and E. Altman, Many-body Landau-Zener dynamics in coupled one-dimensional Bose liquids, Nat. Phys. **7**, 61 (2011).

[36] S. B. Koller, E. A. Goldschmidt, R. C. Brown, R. Wyllie, R. M. Wilson, and J. V. Porto, Nonlinear looped band structure of Bose-Einstein condensates in an optical lattice, Phys. Rev. A **94**, 063634 (2016).

[37] Q. Guan, M. K. H. Ome, T. M. Bersano, S. Mossman, P. Engels, and D. Blume, Non-Exponential Tunneling Due to Mean-Field Induced Swallowtails, Phys. Rev. Lett. **125**, 213401 (2020).

[38] I. Yu. Chestnov, A. V. Yulin, A. P. Alodjants, and O. A. Egorov, Nonlinear Bloch waves and current states of exciton-polariton condensates, Phys. Rev. B **94**, 094306 (2016).

[39] K. G. Makris, R. El-Ganainy, D. N. Christodoulides, and Z. H. Musslimani, Beam Dynamics in $\mathcal{PT}$ Symmetric Optical Lattices, Phys. Rev. Lett. **100**, 103904 (2008).

[40] See Supplemental Material at http://link.aps.org/supplemental/10.1103/PhysRevLett.127.034101 where the two-mode approximation model is provided analytically.

[41] B. Wu and Q. Niu, Landau and dynamical instabilities of the superflow of Bose-Einstein condensates in optical lattices, Phys. Rev. A **64**, 061603(R) (2001).

[42] V. V. Konotop and M. Salerno, Modulation instability in Bose-Einstein condensates in optical lattices, Phys. Rev. A **65**, 021602(R) (2002).

[43] L. Fallani, L. De Sarlo, J. E. Lye, M. Modugno, R. Saers, C. Fort, and M. Inguscio, Observation of Dynamical Instability for a Bose-Einstein Condensate in a Moving 1D Optical Lattice, Phys. Rev. Lett. **93**, 140406 (2004).

[44] C. Hamner, Y. Zhang, M. A. Khamehchi, M. J. Davis, and P. Engels, Spin-Orbit-Coupled Bose-Einstein Condensates in a One-Dimensional Optical Lattice, Phys. Rev. Lett. **114**, 070401 (2015).

[45] M. Stepić, C. Wirth, C. E. Rüter, and D. Kip, Observation of modulational instability in discrete media with self-defocusing nonlinearity, Opt. Lett. **31**, 247 (2006).